Asymmetry of weak photospheric fields in solar cycles 21-24: Implications to magnetic field structure and diffusion

K. Mursula[1], T. Getachew[2], I. Virtanen[3], I. Skokic[4], and R. Brajsa[4]

kalevi.mursula@oulu.fi

[1] Space Climate Research Group, Space Physics and Astronomy Research Unit, University of Oulu, Finland
[2]Department of Astrophysical Sciences, Princeton University, Princeton, NJ, USA
[3]University of Applied Sciences, Oulu, Finland
[4]Hvar Observatory, Faculty of Geodesy, University of Zagreb, Zagreb, Croatia

Background: Importance of weak fields

The weakest magnetic field elements make a dominant contribution to the total magnetic flux on the solar surface.

However, not much is known about the long-term occurrence and evolution of the weakest field elements.

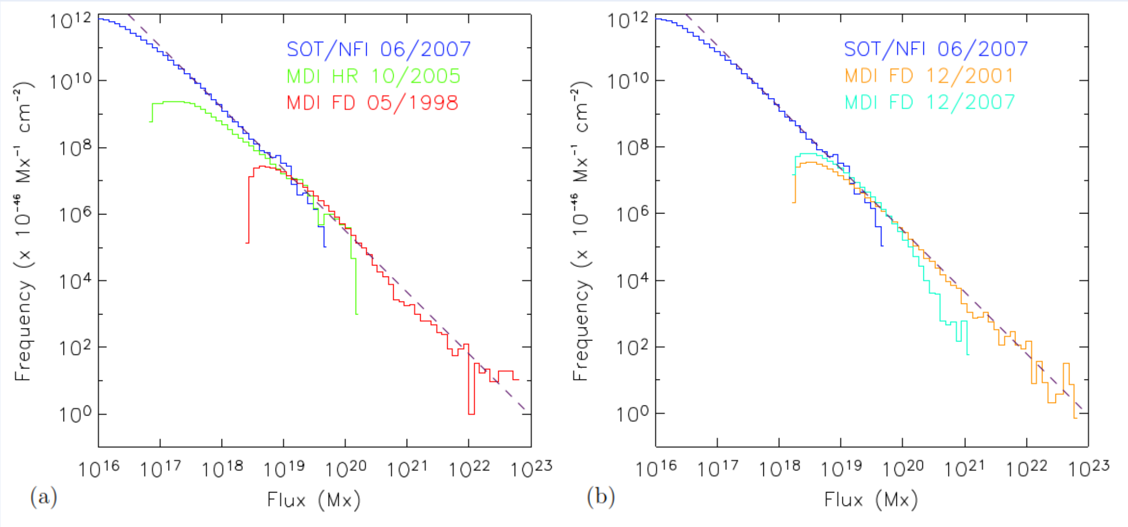

(a) Histograms of fluxes of magnetic features observed in 2007 in Hinode/SOT data (blue), in 2005 in MDI high-resolution data (green), and in 1998 in MDI full-disk data (red).
(b) As (a), with SOT 2007 data (blue) compared with 2001 (orange) and 2007 (cyan) MDI full-disk data.
Dashed line in both graphs is a fit to the data in (a) and has the slope of −1.85 [Parnell et al., 2009].

Background: Weak-field asymmetry

Maximum (peak) of the distribution of the weakest magnetic fields has often seen to be offset from zero.

=> "Zero-level offset"

However, this zero-level offset has mostly been considered to be unphysical and random.

Various methods have been applied to remove it from the observations.
Synoptic maps have typically been ¨purified¨ from zero-level offset.

In a series of papers, we have studied the detailed spatial distribution of the asymmetry of weakest field values ("weak-field (polarity) asymmetry" or "weak-field shift") and its evolution in solar cycles 21-24.

Method

We calculated the histogram distribution (of each synoptic map or only one latitude strip) within $\pm 10G$ (also other limits were used) with a bin size of 0.1 G.

Then we fitted the histogram distribution with a Gaussian function given as:

$$\phi = c * exp\left(-\frac{1}{2}\left(\frac{B_i - a}{b}\right)^2\right)$$

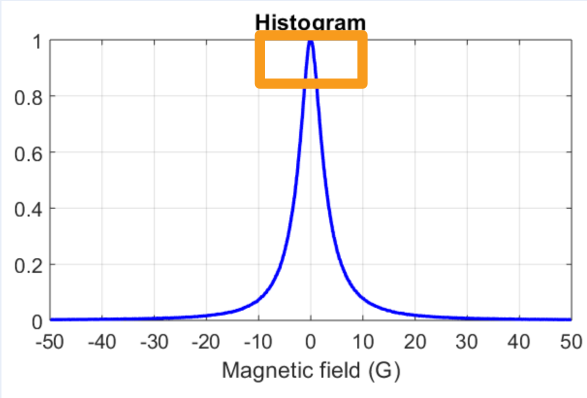

- B_i are field values.
- Parameter a gives the position of the distribution maximum, the weak-field asymmetry.
- Parameters b and c give the width (standard deviation) and the height of the distribution.
- Fit done by least squares (Gauss-Newton) method.
- Statistical significance tested using Student´s t-test.

Synoptic datasets used

UNIVERSITY OF OULU

Instruments	Resolution	Time	Rotation (CR)
WSO	72*30 (F maps)	1976.3 – 2018.8	1642 – 2210
MWO	971*512	1974.5 – 2013.0	1617 – 2131
KPVT	360*180	1975.1 – 2003.7	1625 – 2006
SOLIS/VSM	1800*900	2003.7 – 2017.8	2007 – 2196
SOHO/MDI	3600*1080	1996.4 – 2011.1	1909 – 2104
SDO/HMI	3600*1440	2010.4->	2096->

In addition to these synoptic maps of original resolution produced at the observatories, we also use lower-resolution synoptic maps obtained by block-averaging from the original maps.

Note: This modifies the weak-field distribution and weak-field asymmetry.

Full-map weak-field asymmetries of several datasets

Simultaneous weak-field asymmetries from different data sets with similar resolutions have quite similar values.

This gives strong evidence for the physical nature of the weak-field asymmetry.

Lower resolution maps give larger weak-field asymmetries.
This applies to all the five datasets that we studied.

We have also shown that that the asymmetries are practically independent of the applied range (±10G).

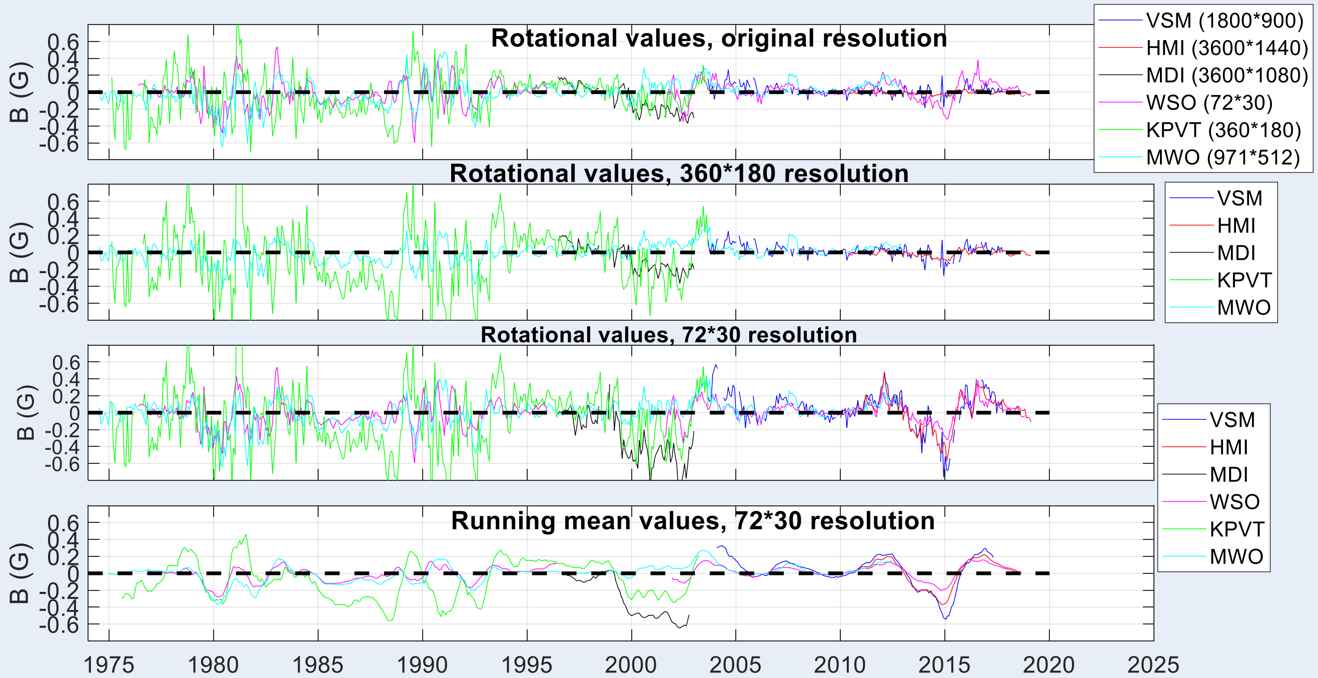

WSO weak-field asymmetry butterfly

UNIVERSITY OF OULU

Spatial-temporal pattern of weak-field asymmetry (weak-field asymmetry butterfly diagram; upper panel) is closely similar to that of all field values (normal butterfly diagram; bottom panel).

The sign (polarity) of the weak-field asymmetry is the same as the polarity of the large-scale field for each surge and for the poles.

Individual surges can be seen even better in the asymmetry butterfly than in the normal butterfly.

Hemispheric asymmetry maximizes during the main surges reaching the pole.

Largest local asymmetries at the poles. However, WSO has poor resolution at high latitudes.

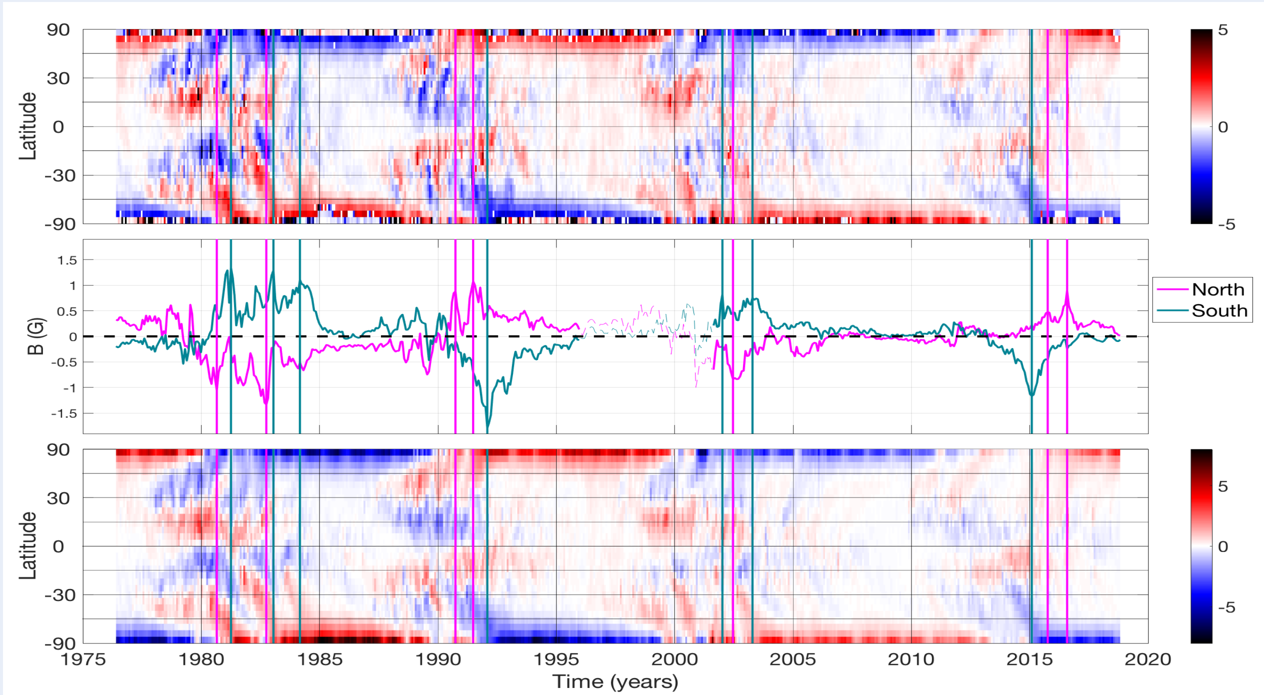

Top: Weak-field asymmetry butterfly diagram (positive in red, negative in blue).
Middle: Hemispheric asymmetry values (north in pink, south in green).
Vertical lines denote their main extrema (north in pink, south in green).
Bottom: Magnetic field butterfly diagram (red positive field, blue negative).

SOLIS weak-field asymmetry butterfly

Large weak-field asymmetry in the polar coronal holes.

Long persistence but no further major increase of asymmetry at the poles.

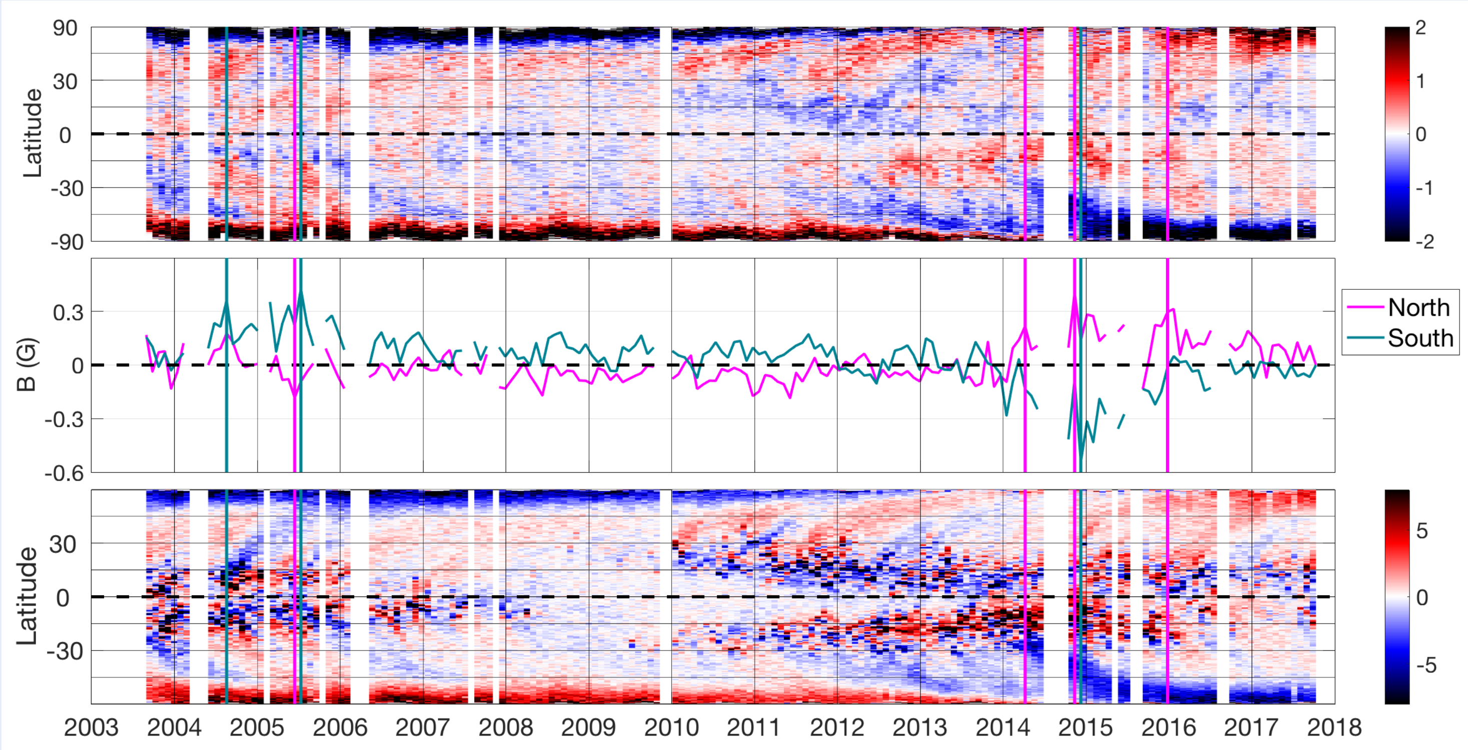

Top: Weak-field asymmetry butterfly diagram (positive shifts in red, negative in blue). Vertical lines denote the shift extrema (north in pink, south in green).
Middle: Hemispheric shift values (north in pink, south in green).
Bottom: Magnetic field butterfly diagram (red positive field, blue negative).

Kalevi Mursula, presentation at ESPM online meeting, 7.9.2021

SOLIS hemispheric weak-field asymmetries

Lower resolution maps give larger weak-field asymmetries.

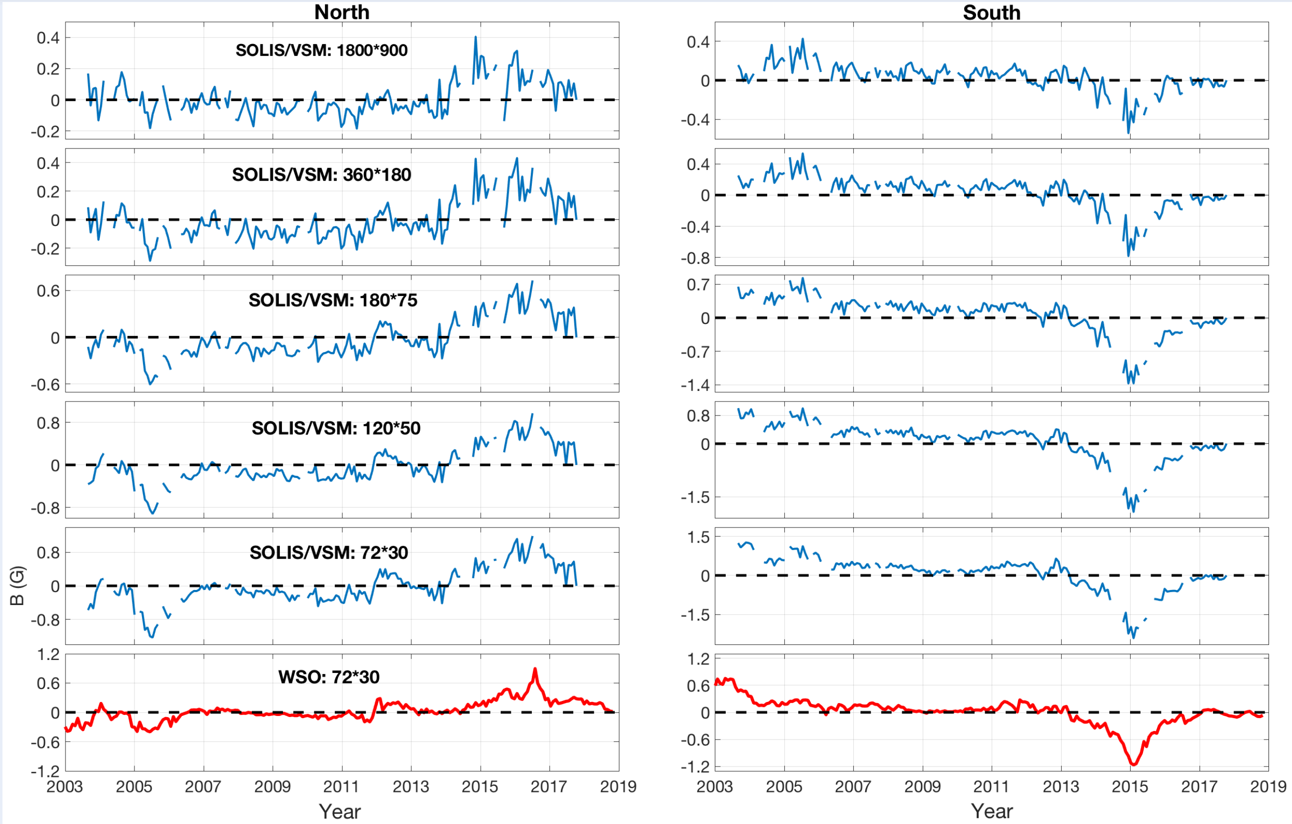

Hemispheric weak-field asymmetries of SOLIS/VSM synoptic map for 1800*900, 360*180, 180*75, 120*50, and 72*30 resolutions.
Left panels: northern hemisphere; *right panels:* southern hemisphere.

SOLIS hemispheric weak-field asymmetries

UNIVERSITY OF OULU

SOLIS WFAs approach WSO WFA as resolution gets lower.

Temporal patterns of WFAs in SOLIS AND WSO agree closely at the same resolution.

The large WFA maxima of the low-resolution maps occur latest, when the surge has reached the pole.

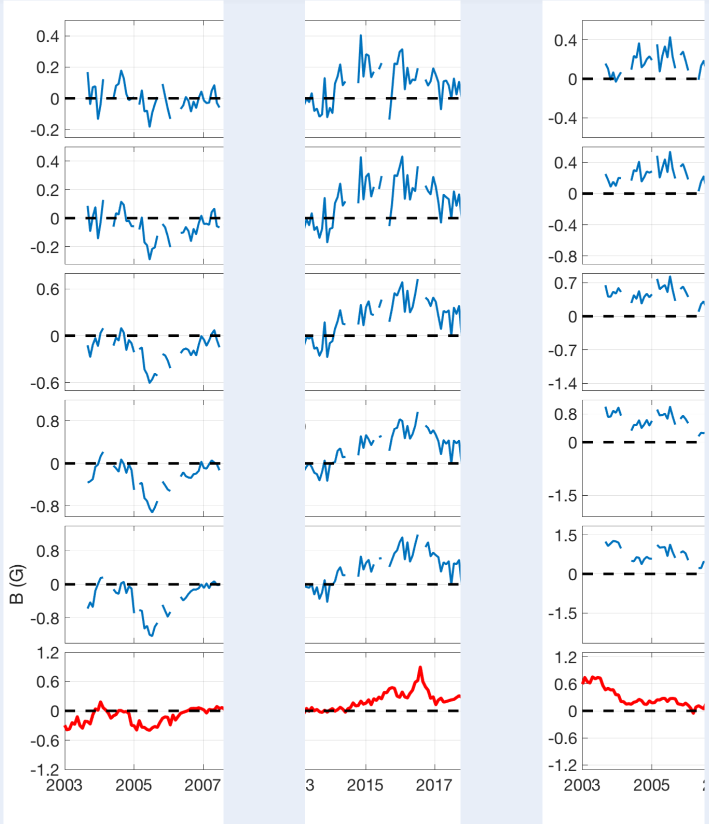

Hemispheric weak-field asymmetries of SOLIS/VSM synoptic map for 1800*900, 360*180, 180*75, 120*50, and 72*30 resolutions.
Left panels: northern hemisphere; *right panels:* southern hemisphere.

SOLIS hemispheric weak-field asymmetries

UNIVERSITY OF OULU

Largest increase in WFA by factor of 2 occurs from 360*180 maps to 180*75 maps (resolution reduction by 4.8).

- Increase from 1800*900 maps to 360*180 maps increase only by 50% (resolution reduction by 25).
- Increase from 180*75 maps to 120*50 maps increase only by 40% (resolution reduction by 6.25).

Note: 180*75 resolution is close to supergranular scale (about 30000km).

Temporal differences in shifts at different resolutions indicate the coalescence of stronger fields during poleward surge to increase the weak-field asymmetry.

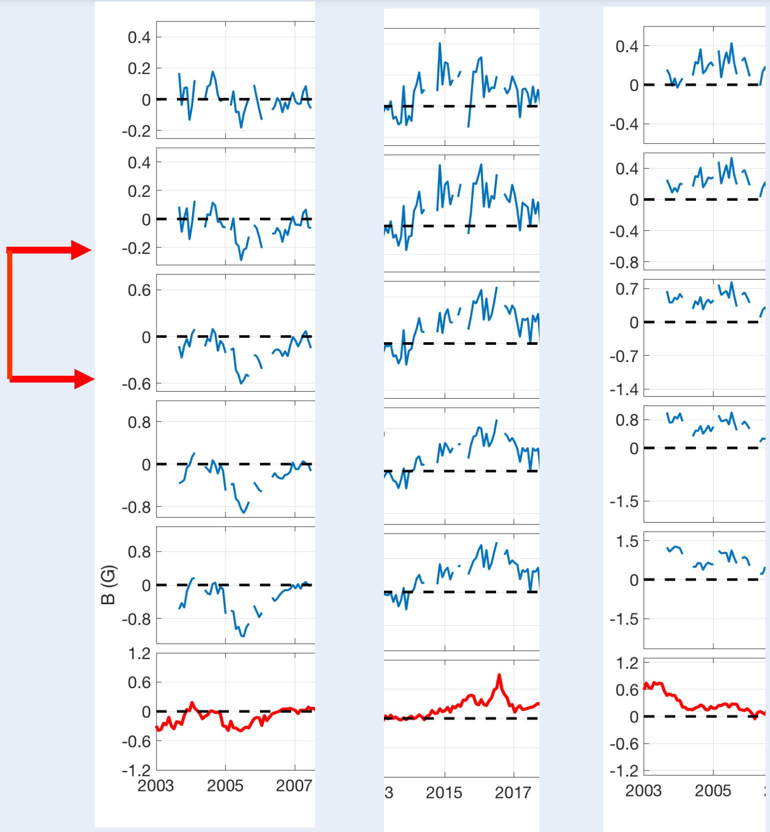

Hemispheric weak-field asymmetries of SOLIS/VSM synoptic map for 1800*900, 360*180, 180*75, 120*50, and 72*30 resolutions.
Left panels: northern hemisphere; *right panels:* southern hemisphere.

SOLIS butterlies for weak-field asymmetry, weak-field skewness and full-field skewness

UNIVERSITY OF OULU

Skewness is the third moment of the distribution function, positive if the data points are spread out more to the positive side of the mean.

Sign (polarity) of the weak-field skewness at the poles is opposite to that of the full-field skewness.

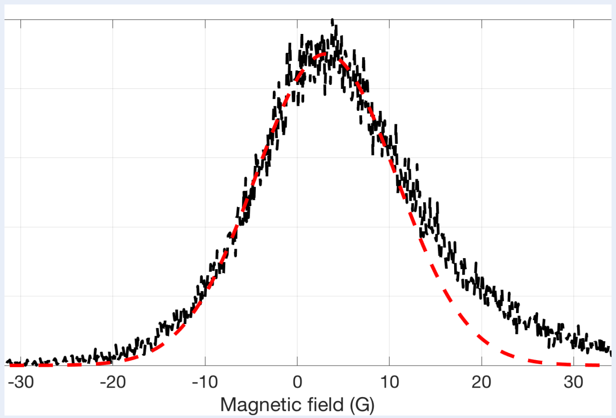

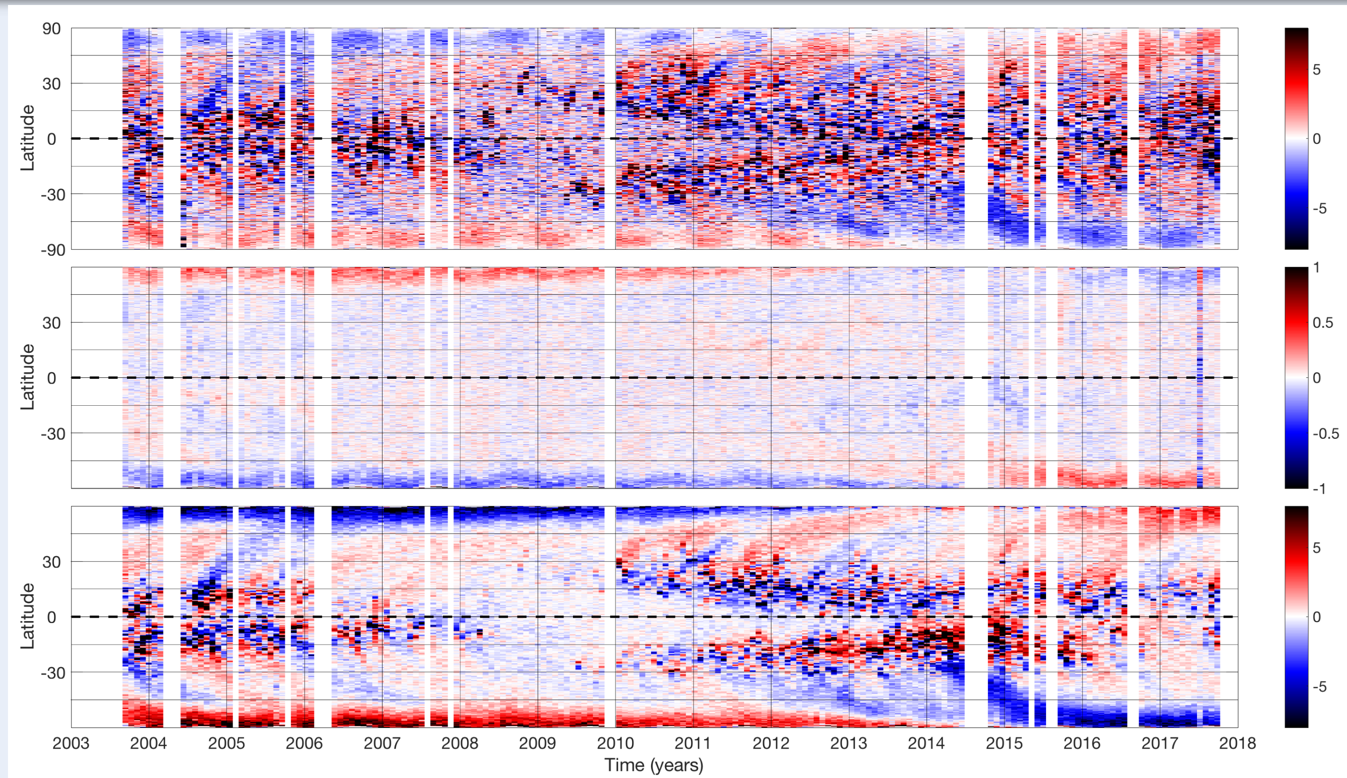

Top: Full-field skewness butterfly diagram (red: positive skewness, blue: negative).
Middle: Weak-field skewness butterfly diagram
Bottom: Magnetic butterfly diagram.

Discussion

UNIVERSITY OF OULU

Maximum of the weak-field distribution is systematically shifted towards the dominant polarity of the surge already at the appearance of the active region.

Low-resolution weak-field asymmetry (WFA) increases during surge evolution toward the pole, indicating coalescence of large, opposite-polarity fields.

Weak-field asymmetry is larger at lower resolution, and the increase when reducing resolution is most effective as the resolution is close to the supergranulation scale.

High-resolution WFA is small during surge but large at the poles.

Low-resolution WFA is large during the surges and at the poles.

Note: There is no scale-dependent difference in WFA at the poles.

This suggests that there is no spatial structure in the unipolar polar regions.

Accordingly, our results suggest a lack or significant **weakening of the supergranulation process at the solar poles.**

Spectral power of CBP motion

There is preliminary evidence that coronal bright point motion is less bounded in the polar coronal hole, as indicated by the larger diffusion spectral index in early 2011 in the southern polar coronal hole.

This would give additional evidence for less effective supergranulation in polar coronal holes.

See Skokic et al., ApJ., 2019.

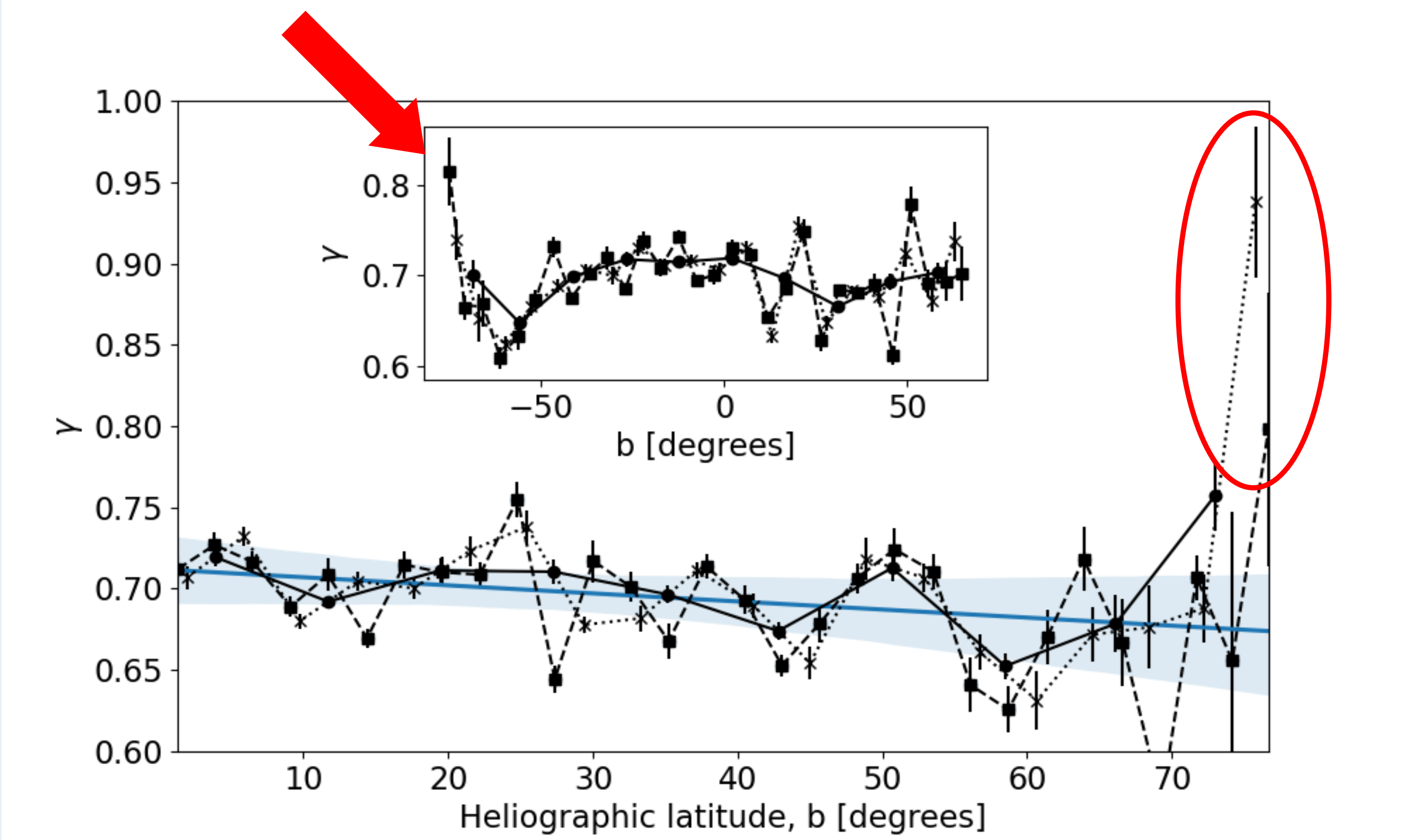

References

- T. Getachew, I.I. Virtanen and K. Mursula, Asymmetric distribution of weak photospheric magnetic field values, Astrophys. J., 874, 116, 10pp, https://doi.org/10.3847/1538-4357/ab0749, 2019.

- I. Skokić, R. Brajša, D. Sudar, D. Ruždjak, and S. H. Saar, Turbulent diffusion derived from the motions of SDO/AIA coronal bright points, Astrophys. J., 877, 142, doi:10.3847/1538-4357/ab1d4f, 2019.

- T. Getachew, I. I. Virtanen and K. Mursula, A new signal of the solar magnetic cycle: Opposite shifts of weak magnetic field distributions in the two hemispheres, Geophys. Res. Lett., 46, 9327-9333, https://doi.org/10.1029/2019GL083339, 2019.

- COPY ATTACHED on ESPM web page:
- K. Mursula, T. Getachew, and I. I. Virtanen, Spatial-temporal evolution of photospheric weak-field shifts in solar cycles 21-24, Astron. Astrophys., 645, A47, 9 pages, https://doi.org/10.1051/0004-6361/201936917, 2021.

Thanks for your interest!

Do not hesitate to contact:

kalevi.mursula@oulu.fi

UNIVERSITY OF OULU